Spectroscopy 17 (2003) 399–416
IOS Press

Structural characterization of the C2 domains of classical isozymes of protein kinase C and novel protein kinase Cε by using infrared spectroscopy

Senena Corbalán-García, Josefa García-García, M. Susana Sánchez-Carrillo and Juan C. Gómez-Fernández *

Departamento de Bioquímica y Biología Molecular (A), Facultad de Veterinaria, Universidad de Murcia, Apartado de Correos 4021, E-30080 Murcia, Spain

Abstract. The amide I regions in the original infrared spectra of PKCα-C2 in the Ca^{2+}-free and Ca^{2+}-bound states are both consistent with a predominantly β-sheet secondary structure. Spectroscopic studies of the thermal denaturation revealed that for the PKCα-C2 domain alone the secondary structure abruptly changed at 50°C. While in the presence of Ca^{2+}, the thermal stability of the protein increased considerably. Phosphatidic acid binding to the PKCα-C2 domain was characterized, and the lipid–protein binding becoming Ca^{2+}-independent when 100 mol% phosphatidic acid vesicles was used. The effect of lipid binding on secondary structure and thermal stability was also studied. In addition, the secondary structure of the C2 domain from the novel PKCε was also determined by IR spectroscopy and β-sheet was seen to be the major structural component. Spectroscopic studies of the thermal denaturation in D_2O showed a broadening in the amide I′ band starting at 45°C. Phosphatidic acid containing vesicles were used to characterize the effect of lipid binding on the secondary structure. It was observed through thermal stability experiments that the secondary structure did not change upon lipid binding and the protein stability was very high with no significant changes occurring in the secondary structure after heating.

1. Introduction

Protein kinase C (PKC) is a phospholipid-dependent serine/threonine kinase family consisting of at least eleven closely related isoenzymes. The different PKC isoenzymes play important roles in signal transduction pathways, although the exact significance of each isoenzyme is not known at present. Any elucidation of the regulation mechanism of the various PKC isoenzymes is therefore important [25].

Closer examination of protein-sequence alignments between PKC isoenzymes reveals blocks of homology between family members and, in every case, these conserved regions have been shown to define protein motifs which confer a specific localization and/or activation input on the isoenzyme [16]. The module composition allows a more precise categorization of the different PKC subfamilies. There are three main classes of PKC molecules: the classical (α, βI, βII, γ) that contain the conserved C1 and C2 motifs in the regulatory domain and which are activated by both Ca^{2+}-dependent phospholipid binding and diacylglycerol; the novel (δ, ε, η, θ, μ), which also contain C1 and C2 motifs, although located in reverse order from those of the classical isoenzymes, and, which are activated by phospholipid and diacylglycerol binding in a Ca^{2+} independent manner; and finally, the atypical isoenzymes (ζ, ι/λ), whose

*Corresponding author. Tel.: +34 968 364766; Fax: +34 968 364766; E-mail: jcgomez@um.es.

regulatory domain does not contain any conserved modules and which are not activated by either Ca^{2+} or diacylglycerol [66].

In general, most of the proteins containing C2-domains function in signal transduction or membrane traffic [26]. Pioneer studies with the C2A-domain of synaptotagmin I revealed that the C2 domain acts as a Ca^{2+} binding motif [6,48,63]. This function has also been demonstrated in several other C2-domain-containing proteins such as classical PKCs [5,40,41,49], cPLA2 [12,43] and Nedd4 [45] all of which bind to phospholipids in a Ca^{2+}-dependent manner. Furthermore, it has recently been found that Ca^{2+} forms a bridge between the C2 membrane-binding domain of PKCα and PS [42]. Moreover, there are many C2-domains that are involved in lipid binding and do not bind Ca^{2+}, as it is the case of the C2 domains from the novel PKCs, the functions of which are still not well characterized [4,11].

X-ray diffraction analysis of several C2 domains has revealed that the structure consists of a compact β-sandwich composed of two four-stranded β-sheets [1,11,17,36,42,44,47,48]. Basically, three loops at the top of the domain and four at the bottom connect the eight β-strands and, interestingly, two distinct but easily interconverted topological folds have been found: topology I becomes topology II when its N- and C-termini are fused and new termini are generated by cutting the loop between strands β1 and β2 [11,26]. The C2 domains of classical PKCs are classified as having a type I topology, while those of novel PKCs exhibit a type II topology [11]. The existence of two topologies is a still unsolved question and, in spite of some studies, it is not clear why C2 domains occur in two modes. As mentioned above, novel PKCs present a unique type of C2 domain and, differently to classical PKCs or phospholipases, they are able to bind to acidic phospholipids in a Ca^{2+}-independent manner. So far, very little is known about the lipid binding mechanism of these isoforms.

In the present work, we have used FT-IR to study in solution the secondary structure of the C2 domain of PKCα during Ca^{2+} and lipid binding independently, and that of the C2 domain of PKCε in the present and in the absence of phosholipid and we have carried out thermal denaturation studies. Infrared spectra are known to report directly on the secondary structure of the protein backbone [18,32,51]. The technique is of particular value in structural studies of membrane or lipid-associated proteins [8,50,59,65]. Our results show that the secondary structure of the C2 domain of PKCα does not change with Ca^{2+} binding. On the contrary, binding to lipids produces significant conformational changes in the secondary structure of the C2 domain. The thermal denaturation studies revealed that both Ca^{2+} and lipid binding increase the stability of the complexes but by means of different mechanisms. In addition we have observed that the structural components of the C2-domain from PKCε show several differences from the C2 domain of PKCα and these differences might be attributed to different structural motifs.

2. Materials and methods

2.1. Construction of expression plasmids

The DNA fragment corresponding to the C2 domains of PKCα (residues 158–285) and PKCε (residues 6 to 134) were amplified using PCR. The PKCs cDNA were a kind gift from Drs. Nishizuka and Ono (Kobe University, Kobe, Japan). The resulting PCR fragment were subcloned using sites of the bacterial expression vectors, pET28, in which the inserts were fused to 6His tag, respectively as described previously [23,24]. All constructs were confirmed by DNA sequencing.

2.2. Expression and purification of the His-PKC-C2 and GST-PKC-C2 domains

The pET28(+) plasmid containing the wild-type or mutant PKCα-C2 domains and the pET28a(+) plasmid containing the PKCε-C2 domain were transformed into BL21(DE3) *Escherichia coli* cells.

The bacterial cultures (OD_{600} 0.6) were induced for 5 h at 30°C with 0.5 mM of isopropyl-1-thio-β-D-galactopyranoside (IPTG) (Boehringer Mannheim, Germany). The cells were lysed by sonication in lysis buffer (25 mM HEPES, pH 7.4, and 100 mM NaCl) containing protease inhibitors (10 mM benzamidine, 1 mM PMSF and 10 μg/ml of trypsin inhibitor). The soluble fraction of the lysate was incubated with Ni-NTA Agarose (QIAGEN, Hilden, Germany) for 2 h at 4°C. The Ni beads were washed with lysis buffer containing 20 mM imidazole. The bound fractions were eluted with the same buffer containing 50, 250 and 500 mM imidazole. 6His tag was removed after thrombin cleavage and, finally, the PKC-C2 domains were desalted and concentrated using an Ultrafree-5 centrifugal filter unit (Millipore Inc., Bedford, MA).

2.3. Preparation of lipid vesicles

Lipid vesicles were generated by mixing chloroform solutions of 1-palmitoyl-2-oleoyl-*sn*-glycero-3-phosphocholine (phosphatidylcholine) (Avanti Polar Lipids, Inc., Alabaster, AL) and 1-palmitoyl-2-oleoyl-*sn*-glycero-3-phosphate (POPA) (Avanti Polar Lipids, Inc., Alabaster, AL) at the desired proportions and dried from the organic solvent under a stream of nitrogen and then further dried under vacuum for 60 min.

2.4. IR spectroscopy

Lyophilized PKC-C2 domains were dissolved in H_2O or D_2O at approximately 20 and 8 mg/ml, respectively. The proteins were incubated overnight at 4°C to maximize H–D exchange when D_2O was used. To study infrared amide bands of the proteins in the presence of lipids, small unilamellar vesicles in D_2O or H_2O buffer containing 25 mM HEPES, 20 mM NaCl and 0.2 mM EGTA, pH 7.4, were mixed in the desired proportions with the protein solution.

Infrared spectra were recorded using either a Bruker Vector 22 Fourier transform infrared spectrometer equipped with a MCT detector or a Philips PU9800 Fourier transform infrared spectrometer equipped with a deuterated triglycine sulfate detector. Samples were examined in a thermostated Specac 20710 cell (Specac, Kent, UK) equipped with CaF_2 windows and 6 μm spacers for samples in H_2O medium or 50-μm spacers for samples in D_2O medium. The spectra were recorded after equilibrating the samples at 25°C for 20 min in the infrared cell. A total of 128 scans were accomplished for each spectrum with a nominal resolution of 2 cm^{-1} and then Fourier transformed using a triangular apodization function. A sample shuttle accessory was used to obtain the average background and sample spectra. The sample chamber of the spectrometer was continuously purged with dry air to prevent atmospheric water vapor obscuring the bands of interest. Samples were scanned between 25 and 75°C at 5°C intervals with a 5-min delay between each scan using a circulation water bath interfaced to the spectrometer computer. Spectral subtraction was performed interactively using the Spectra-Calc program (Galactic Industries Corp., Salem, NH). The spectra were subjected to deconvolution and second-derivation using the same software. Fourier self-deconvolution was carried out using a bessel apodization function, a Lorentzian shape with a resolution enhancement parameter, K, of 2.6 and a full width at half-height of 20 cm^{-1}. Both deconvolution and derivation gave the number and position, as well as an estimation of the bandwidth and intensity of the bands making up the amide I region. Thereafter, curve-fitting was performed and the heights, widths and positions of each band were optimized successively [29,31]. The fractional areas of the bands in the amide I region were calculated from the final fitted band areas.

3. Results and discussion

3.1. Structure of the C2 domain of PKCα

The amide I band decomposition of the native PKCα-C2 domain in D_2O and 0.2 mM EGTA at 25°C is shown in Fig. 1. The number and initial position of the component bands were obtained from band-narrowed spectra by Fourier deconvolution and derivation. The corresponding parameters, e.g. band position, percentage area, bandwidth of each spectral component and assignment, are shown in Table 1 for

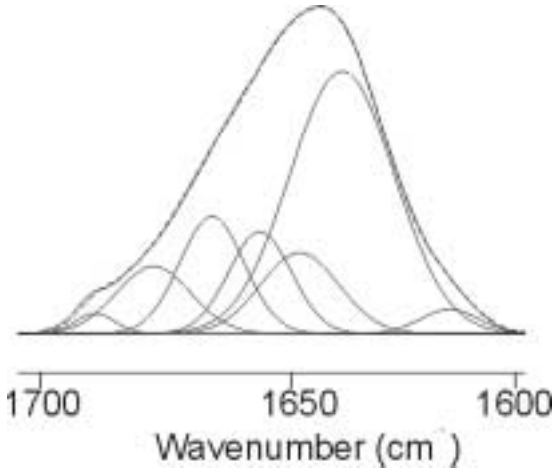

Fig. 1. FT-IR spectrum of PKCα-C2 domain in the amide I region at 25°C in D_2O buffer (solid line) with the fitted component bands. The position of the individual band was obtained from the resolution-enhanced spectrum. The parameters corresponding to the component bands are reflected in Table 1. Dashed line, curve fitted spectrum. Protein concentration was approximately 16 mg/ml. Increment of absorbance units (Δ) were 0.05. Reproduced with permission from *Biochemistry* **38** (1999), 9667–9675. Copyright 1999 Am. Chem. Soc.

Table 1

FT-IR parameters of the amide I band components of PKC-C2 domain in D_2O buffer containing 25 mM HEPES and 0.2 mM EGTA, 2 mM and 12.5 mM Ca^{2+}, pD 7.4. Reproduced with permission from *Biochemistry* **38** (1999), 9667–9675. Copyright 1999 Am. Chem. Soc.

Position[a] (cm^{-1})	Assignment	25°C						75°C		
		0.2 mM EGTA		2 mM Ca^{2+}		12.5 mM Ca^{2+}		0.2 mM EGTA		
		Area[b] (%)	Width[c] (cm^{-1})	Area (%)	Width (cm^{-1})	Area (%)	Width (cm^{-1})	Position (cm^{-1})	Area (%)	Width (cm^{-1})
1688	β-turns	1	12	2	12	3	13	1680	11	19
1675	Antiparallel β-sheet	9	22	8	21	7	17	1670	13	13
1663	β-turns	14	19	14	19	16	18	1663	14	20
1652	α-helix/turns with dihedral angles similar to α-helix	12	19	12	19	14	17	1647	34	28
1644	Random/ open loops	12	24	13	24	9	19	1631	16	22
1635	β-sheet	51	32	50	32	51	31	1615	23	19

[a]Peak position of the amide I band components.
[b]Percentage area of the band components of amide I. The areas corresponding to side-chain contributions located at 1615–1600 cm^{-1} have not been considered.
[c]Half bandwidth of the amide I components. The values are rounded off to the nearest integer.

both H_2O and D_2O. The spectra in H_2O showed six components in the amide I region. The main component accounting for 50% of the total band area was localized at 1639 cm^{-1} and it can be assigned to β-structure [28]. The component localized at 1657 cm^{-1} which contributes a 22% of the total area may be assigned to either α-helix or disordered structure [28]. The components appearing at 1678 cm^{-1} (8%) and 1668 cm^{-1} (11%) arise from β-turns [20,21] and the component centered at 1688 cm^{-1} (11%) was assigned to antiparallel β-sheet [28]. On the other hand, the component at 1616 was supposed to be originated from the absorption of lateral chains and hence it was not taken into account for the quantification of the different types of secondary structure. In summary the secondary structure of the C2 domain of PKCα in H_2O was 59% β-pleated sheet, after adding the areas of components at 1639 and 1688 cm^{-1}, 22% assigned to α-helix, open loops and disordered structures and 19% β-turns (Table 1).

The spectra in D_2O exhibit seven component bands in the 1700–1600 cm^{-1} region and the quantitative contribution of each band to the total amide I contour, obtained by band curve-fitting of the original spectra are shown in Table 1. The major component in the amide I′ region appears at 1635 cm^{-1}, and so clearly arises from intramolecular C=O vibrations of β-sheets [14,19,29,31,37,51] and corresponds to the band appearing at 1639 cm^{-1} in H_2O buffer. The high frequency component at 1675 cm^{-1} can be assigned to the antiparallel β-sheet structure [3,31]. Although α-helix usually absorbs at around 1652 cm^{-1}, bands originating from turns, with dihedral angles comparable to those of α-helix, have also been described at this frequency [21,31,51]. The band near 1644 cm^{-1} can be attributed to non-structured conformations, including open loops [14,18]. The bands located at 1663 cm^{-1} and 1688 cm^{-1} arise from β-turns [3,32]. Additionally, there is a band at about 1612 cm^{-1}, which has been assigned to side chain absorption [18,21,22], and so, its contribution is not included in the calculation of the secondary structure of PKC-C2. The secondary structure of PKCα-C2 domain (Table 1) is 60% β-sheet (taking into account the 1635 and 1675 cm^{-1} bands), 12% α-helix/dihedral turns (similar to α-helix), 15% β-turns and 12% open loops and non-structured conformation.

It is interesting to compare here the results obtained through spectra taken in the presence of H_2O and D_2O. One of the advantages of obtaining spectra in D_2O is that it is allowed to discern between the components corresponding to α-helix and disordered structure which however appeared unresolved in H_2O buffer. The data shown present a good correlation between the spectra taken in both type of solvents. They present 60% (D_2O) and 59% (H_2O) for β-sheet, 24% for the addition of α-helix and disordered structure in D_2O (adding components at 1652 and 1644 cm^{-1}) versus 22% in H_2O and finally 15% and 18% for β-turns in D_2O and H_2O, respectively.

Another interesting comparison to be made is between the secondary structure composition deduced from infrared spectroscopy (this paper) and from X-ray diffraction (XRD) [42]. Table 2 shows that the agreement was strikingly good between both techniques with β-structure amounting to 60 and 57% for IR (in D_2O) and XRD respectively, α-helix plus big loops being 125 for both techniques, β-turns amounting to 15 and 16% for IR and XRD, respectively, and disordered structure plus open loops 12 and 14% for IR and XRD, respectively.

3.2. Effect of Ca^{2+}-binding on the structure and stability of C2 domain of PKCα

Although it has been demonstrated previously that the PKCα-C2 domain is involved in Ca^{2+} binding, it is not clear whether this binding affects the conformation of the protein. We studied the effect of Ca^{2+} binding on the secondary structure of the PKCα-C2 domain using 2 and 12.5 mM $CaCl_2$, which, in the conditions of the assay represent Ca^{2+}/protein ratios of 2 : 1 and 14 : 1, respectively. Based on the binding assays performed by Nalefski et al. [12] for the C2 domain of cytosolic phospholipase A2, the higher

Table 2
FT-IR parameters of the amide I band components of the PKCα-C2 domain in H_2O buffer containing 25 mM Hepes, 0.2 mM EGTA and 12.5 mM Ca^{2+} (pH 7.4)

	Area (%)	Width (cm^{-1})	Maximum (cm^{-1})
β-sheet	50	32	1639
α-helix and large loops and random	22	23	1657
β-turns	11	19	1668
β-turns	8	21	1678
Antiparallel β-sheet	9	27	1688

concentration would produce maximal binding, while 2 mM is a non-saturating concentration under the conditions of the FT-IR experiment. The spectra of the protein at 25°C in the presence of 2 and 12.5 mM $CaCl_2$ both look very similar to that described above for the protein in the absence of $CaCl_2$ (not shown here, see García-García et al. [24]), including the number and position of the amide I component bands. There is only a component at 1644 cm^{-1} which shows a significant decrease at 12.5 mM $CaCl_2$ going down to 9% whereas it was 13% in the absence of Ca^{2+}.

Further insight into the structural changes that occur during ligand binding was obtained from thermal stability studies. The deconvolved FT-IR spectra of the PKCα-C2 domain in D_2O/EGTA buffer revealed major changes in the amide I mode between 50 and 65°C (Fig. 2A). These changes included a broadening of the overall amide I contour and the appearance of well defined components at 1615 and 1680 cm^{-1}, which is highly characteristic of thermally denatured proteins [29,58]. These components indicate that extended structures were formed by aggregation of the unfolded proteins, which were produced as a consequence of irreversible thermal denaturation [31,58]. It is also remarkable to note that apart from the appearance of the 1615 and 1680 cm^{-1} components, other changes in the structure resulted from protein denaturation. The spectrum corresponding to 55–75°C shows a 1647 cm^{-1} band as the major component, which corresponds to an unordered structure and represents 34% of the total area (Table 1). The band at 1631 cm^{-1} corresponds to a β-sheet structure and shows two main changes: the percentage of the total area has decreased to 16%, and the maximum wavelength of this component has shifted from 1635 cm^{-1} at 25°C to 1631 cm^{-1} at 75°C (Fig. 2B). Thus, thermal denaturation of the PKCα-C2 domain is characterized by irreversible aggregation and unfolding of the β-sheet structure into a disordered structure.

Figure 3 shows the effect of non-saturating (2 mM) and saturating (12.5 mM) Ca^{2+} on the thermal denaturation of the PKCα-C2 domain. The addition of 2 mM Ca^{2+} increases the temperature at which thermal denaturation occurs from 55°C to 65°C (Fig. 3A) and the final effect was very similar to that obtained in the absence of Ca^{2+} (compare to Fig. 2A). However, with 12.5 mM $CaCl_2$ the whole process is shifted to higher temperatures (Fig. 3B), indicating that the domain has a higher stability when bound to Ca^{2+}. The half-midpoint temperature of thermal denaturation was calculated to be about 52–53°C when EGTA was used, 59–60°C in the presence of 2 mM Ca^{2+} and above 70°C in the presence of 12.5 mM Ca^{2+} [24].

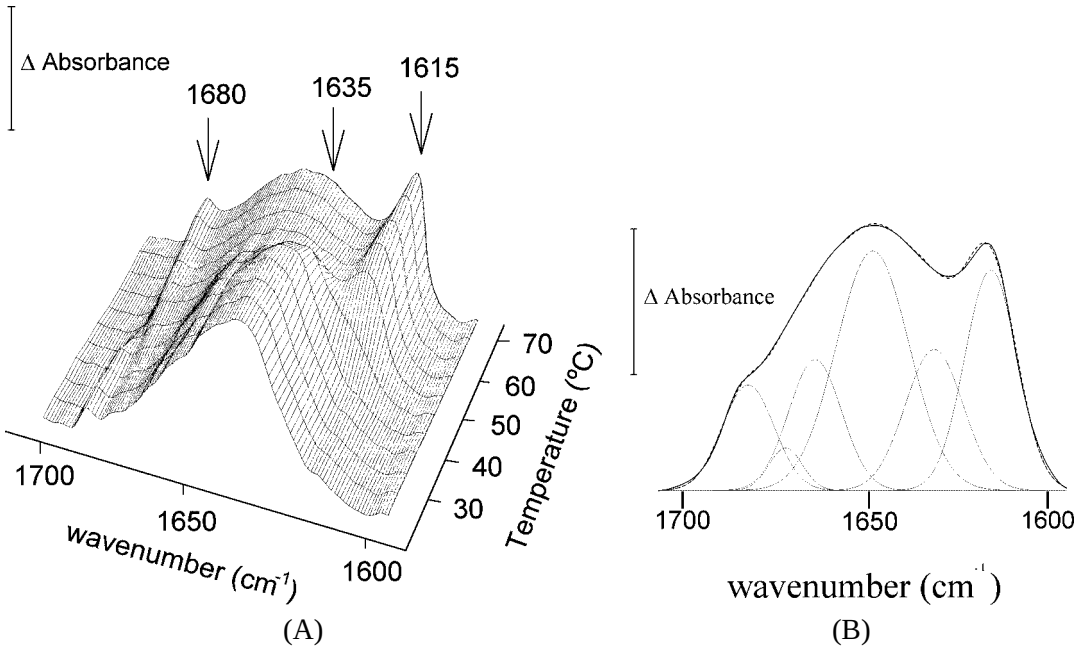

Fig. 2. (A) Deconvolved FT-IR spectrum of PKC□-C2 domain in D_2O buffer containing 0.2 mM EGTA in the amide I region (1700–1600 cm^{-1}) as a function of temperature from 25 to 75°C. Fourier self-deconvolution was carried out using a Lorentzian line-shape, a bandwidth of 18 cm^{-1} and a resolution enhancement factor of 2.4. (B) Amide I band decomposition of thermally denatured PKCα-C2 domain at 75°C. Increment of absorbance units (Δ) were 0.05. The parameters corresponding to the component bands are reflected in Table 1. Reproduced with permission from *Biochemistry* **38** (1999), 9667–9675. Copyright 1999 Am. Chem. Soc.

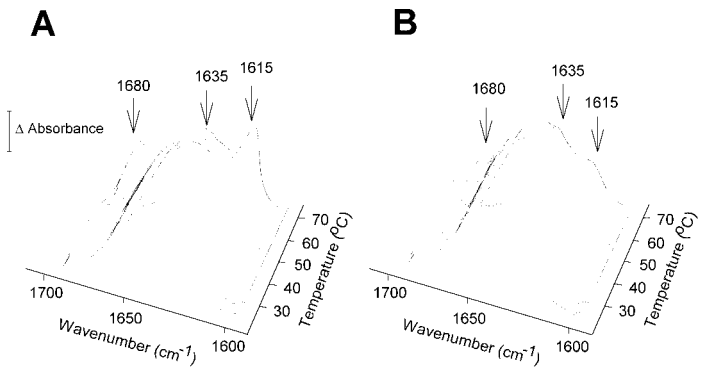

Fig. 3. Deconvolved FT-IR spectrum of PKC□-C2 domain in D_2O buffer containing 2 mM Ca^{2+} (A) and 12.5 mM Ca^{2+} (B) in the amide I region (1700–1600 cm^{-1}) as a function of temperature from 25 to 75°C. Increment of absorbance units (Δ) were 0.05. Reproduced with permission from *Biochemistry* **38** (1999), 9667–9675. Copyright 1999 Am. Chem. Soc.

To further demonstrate that Ca^{2+} is involved in conferring a higher stability against thermal denaturation to the PKCα-C2 domain, we used a construct which contains two mutations from Asp246/248 to Asn (PKCα-C2-D246/248N) and that is not able to bind Ca^{2+} [49]. The FT-IR spectrum at 25°C was very similar to that of PKCα-C2. Thermal denaturation experiments were performed under the same conditions described above for wild type protein, and it was found that when the mutant was incubated in the presence of EGTA, the denaturation pattern showed higher stability with a transition temperature

of 64–65°C. Maximal denaturation was reached at 70°C, as with the wild type PKCα-C2 domain. However, when Ca^{2+} was added at concentrations of 2 and 12.5 mM [24] thermal stability was unaffected, and the transition temperature remained constant at 64–65°C, suggesting that Ca^{2+} binding is important for stabilization, and demonstrating that Ca^{2+} does not stabilize the protein structure of this mutant as it does the structure of the wild type.

X-ray studies of this C2 domain have shown an eight-stranded antiparallel β-sandwich involving 60% of the amino acidic residues [42]. These β-sheets are connected by several turns and three loops. Loops 1 and 3 are involved in Ca^{2+} binding in C2 domains of topology I. In particular, the crystal structure of the C2 domain of PKCα has revealed three Ca^{2+} binding sites [56]. All three sites appear to be hexacoordinate or heptacoordinate, with Ca^{2+}-ligand coordination distances ranging from 2.4–2.6 Å. Our FT-IR studies on the free-state PKCα-C2 domain also show antiparallel β-sheets as the major structure (Fig. 1 and Table 1). In the presence of Ca^{2+}, no changes in the secondary structure were observed (Fig. 2 and Table 1). These data correlate well with other data previously obtained for the C2 domain of synaptotagmin I, where Ca^{2+} binding only involves rotations of some side chains but causes no substantial backbone rearrangement [63,64].

Thus, from the data obtained above, we can conclude that Ca^{2+} does not induce a major change in the secondary structure of the C2 domain of PKCα. However, it is still not clear how Ca^{2+} regulates the C2 domain function. When further information on the effect of Ca^{2+} on the C2 domain was sought using thermal denaturation studies and site-directed mutagenesis, we found that the denaturation mechanism involves irreversible aggregation and unfolding of the scaffold β-sandwich. Ca^{2+} binding stabilized the protein–Ca^{2+} complex during thermal denaturation and the half-midpoint of denaturation temperature shifted from 50 to 60°C at 2 mM Ca^{2+} and to approximately 70°C at 12.5 mM Ca^{2+} [24]. Similar results were obtained by circular dichroism for the C2 domain of synaptotagmin I, where Ca^{2+} binding induced a shift in the denaturation temperature from 55°C to 74°C [63].

Studies performed with PKCα-C2D246/248N mutant revealed that these two mutations of Asp 246 and Asp 248 to Asn are capable of producing by themselves an increase in the domain's stability during thermal denaturation, when the transition temperature shifted from 52 to 64°C. This temperature shift is very similar to that obtained when a non-saturating Ca^{2+} concentration was used. Taking into account that we only mutated two of the five residues involved in Ca^{2+} binding, these results indicate that neutralization of the negative charges existing in this crevice, either by Ca^{2+} binding or substitution of Asp residues by Asn, is an important mechanism for stabilizing the protein. Thus, these data confirm that, at least in the case of the C2 domain of PKCα, while Ca^{2+} does not induce a major conformational change, it does produce a structural stabilization that could account for Ca^{2+} regulation, and might modulate the interaction of the domain with acidic lipids.

3.3. Effect of lipid binding on the PKCα-C2 domain

FT-IR was used to characterize the effect of PKCα-C2 domain's binding to phosphatidic acid on its secondary structure in the absence of Ca^{2+}. It was observed [24] that the effect of the lipid on the secondary structure was significant (Table 3) so that the secondary structure composition for the PKCα-C2 domain bound to phosphatidic acid vesicles yielded values of 47% β-sheet, 21% random, 14% α-helix/dihedral turns similar to α-helix and 17% β-turns. It is interesting to note this effect of lipids on the secondary structure of the PKCα-C2 domain, especially the decrease in the β-sheet component from 60 to 47% and the increase in the component assigned to random and open loops structure from 12 to 21%, when comparing with protein in the absence of lipids (Table 1).

Table 3
Comparison of the composition (%) of the secondary structure obtained from infrared spectroscopy and from X-ray diffraction of the C2-domains from PKCα and from PKCε

Structure	C2-PKCα		C2-PKCε	
	FT-IR (%)	X-ray diffraction (%)	FT-IR (%)	X-ray diffraction (%)
β-sheet	60	57	60	54
α-helix and large loops	12	12	21	20
β-turns	15	16	19	20
Random and open loops	12	14		

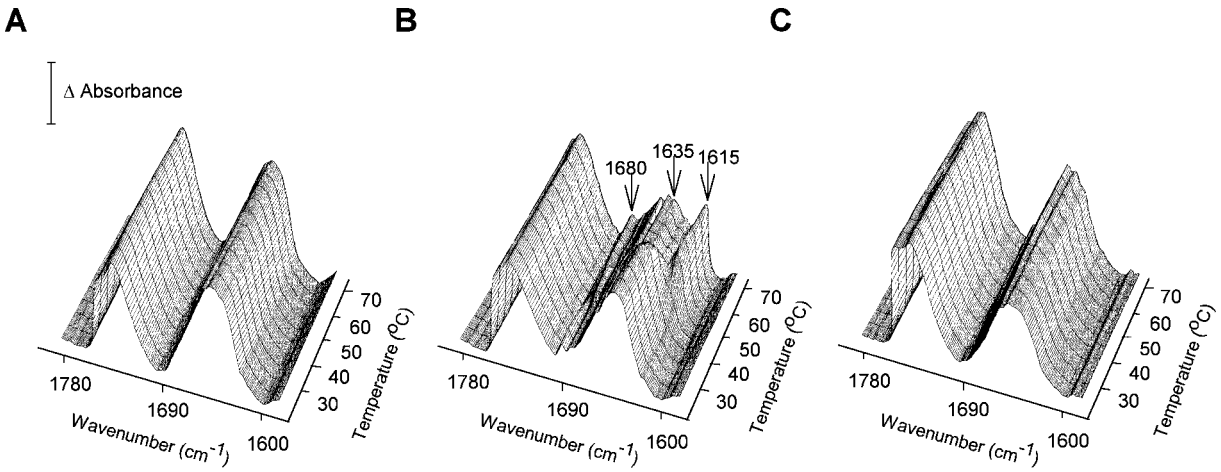

Fig. 4. Deconvolved FT-IR spectrum of PKCα-C2 domain in the presence of lipidic vesicles in the 1800–1600 cm^{-1} region obtained at different temperatures. Phosphatidic acid vesicles were incubated with PKCα-C2 domain (A) phosphatidylcholine vesicles and PKCα-C2 domain were used as control (B) and PKCα-C2D246/248N (C). Increment of absorbance units (Δ) were 0.1. Reproduced with permission from *Biochemistry* **38** (1999), 9667–9675. Copyright 1999 Am. Chem. Soc.

We have previously demonstrated that the mutant PKCα-C2D246/248N binds phosphatidic acid although is not able to bind Ca^{2+} [24]. The percentages of components obtained after band decomposition of the amide I band of this mutant in the presence of vesicles containing 100 mol% phosphatidic were also obtained, and it was interesting that the percentages of the β-sheet and unordered structure components changed as with wild type protein, which confirms the binding of the domain to lipid vesicles in these conditions in which Ca^{2+} was not present.

The binding site for phosphatidic acid, in the absence of Ca^{2+} must take place on the lysines-rich cluster located in β-strands 3 and 4 where it has recently been observed that phosphatidic acid binds. Several studies have shown that activation of classical PKCs involves conformational changes, including the removal of the pseudosubstrate region from the active site of PKC [60,61]. Thus, ours results suggest that the C2 domain might also be involved in this conformational change during lipid binding which leads to protein activation

The effect of heating on the structure of PKCα-C2 in the presence of phosphatidic acid was also studied by FT-IR (Fig. 4). In the presence of lipid vesicles containing 100 mol% phosphatidic acid, PKCα-C2 did not change its FT-IR profile significantly in the temperature range tested, suggesting a large increase in

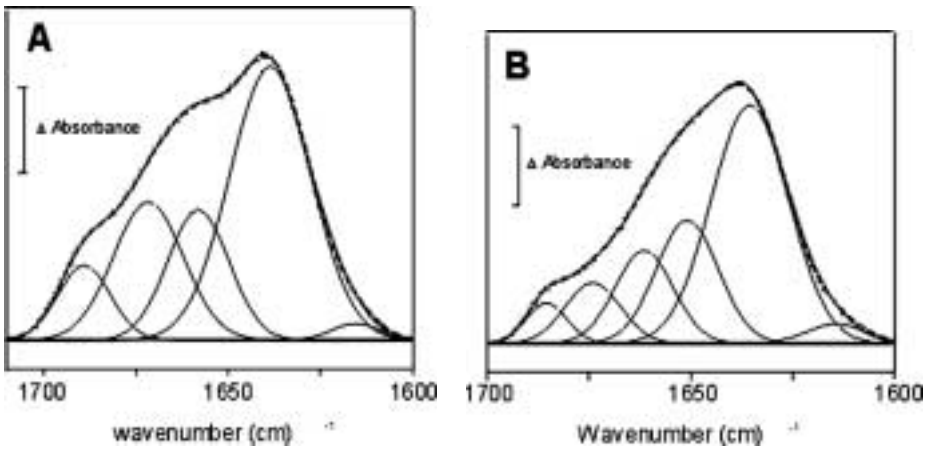

(A) (B)

Fig. 5. Amide I band decomposition of the PKCε-C2 domain in H_2O (A) and D_2O (B) at 25°C. The position of the individual bands was obtained from the resolution-enhanced spectra represented in Fig. 2. The parameters corresponding to the component bands are reflected in Table 1. The dashed line represents the curve-fitted spectra. The increment of absorbance units (Δ) was 0.02 (A) and 0.1 (B). Reproduced with permission from *Eur. J. Biochem.* **268** (2001), 1107–1117. Copyright 2001 Blackwell Sci.

stability. As a control, we performed the same assay using PKCα-C2 and 100 mol% phosphatidylcholine vesicles and no binding occurred. In this case, PKCα-C2 underwent thermal denaturation with a half-midpoint temperature of 52–53°C (Fig. 4B), exactly the same temperature as in the absence of lipids (see Fig. 2A). Figure 4C shows the effect of thermal denaturation on the stability of the PKC-C2D246/248N mutant and as can be appreciated, a big increase in the stability of the protein occurred with lipid binding, confirming that the protein had bound to the lipid vesicles. These data suggest that the amino acidic residues involved in lipid binding are, at least in part, different from those involved in Ca^{2+} binding. Furthermore, lipid interaction led to a very high degree of protein structure stabilization and no change in secondary structure was detected even after heating to 70°C.

Thermal denaturation studies of PKCα-C2–phosphatidic acid complexes reveal the very high stability of the protein compared with its free-Ca^{2+} and bound-Ca^{2+} states, indicating that thermal denaturation does not occur in these conditions, at least in the temperature range studied. This high stability is similar to that described for intrinsic membrane proteins [50,65].

3.4. Structure of the PKCε-C2 domain

To study the structure of the C2 domain of PKCε (PKCε-C2), a recombinant fusion protein was generated and purified as described in the Experimental procedures section. Protein structure was studied by analyzing the amide I region of the infrared spectrum both in H_2O and in D_2O. Deconvolution of the spectrum obtained in H_2O-buffer showed four components and similar results were found after obtaining the second derivative spectrum. Five components were found when the D_2O spectrum was submitted to deconvolution and second derivation. Quantitation was carried out by curve fitting to the original spectra (Fig. 5). The corresponding parameters, i.e. band position, percentage area, and bandwidth of each spectral component are displayed in Table 4. In the H_2O spectrum, the main component was centered at 1639 cm^{-1} and amounted to 51%. This wavelength can be attributed to β-sheet structure [31], the major structural component of C2 domains [11,26]. The component at 1658 cm^{-1}, which amounted to 18%,

Table 4

FT-IR parameters of the amide I band components of PKCα-C2 and PKC-C2D246/248N domains in the absence or presence of small unilamellar vesicles containing 100 mol% phosphatidic acid, in 0.2 mM EGTA D_2O buffer at 25°C. Reproduced with permission from *Biochemistry* **38** (1999), 9667–9675. Copyright 1999 Am. Chem. Soc.

PKCα-C2			PKCα-C2D246/248N					
Phosphatidic acid			No lipid			Phosphatidic acid		
Position (cm^{-1})	Area (%)	Width (cm^{-1})	Position (cm^{-1})	Area (%)	Width (cm^{-1})	Position (cm^{-1})	Area (%)	Width (cm^{-1})
1693	<1	11	1688	3	14	1693	1	14
1677	8	19	1675	7	17	1677	10	22
1663	17	19	1663	17	18	1662	23	22
1653	14	17	1653	11	15	1652	12	16
1644	21	20	1645	9	17	1643	18	19
1631	39	28	1635	53	31	1631	35	29

is usually assigned to α-helix and/or unordered structures [28] but could also be assigned to large loops with dihedral angles similar to those of α-helix [7,53,54,57]. The component at 1671 cm^{-1}, amounting to 22%, is assigned to β-turns [20,21]. Finally the band at 1689 cm^{-1}, which can be assigned to the high frequency component of antiparallel β-sheet in the case of proteins in H_2O solution [28] amounted to 9% of the total area.

When the protein was studied in D_2O, five components were basically detected both by deconvolution and derivation (Fig. 5). The band centered at 1636 cm^{-1} corresponds to a β-sheet structure and was the main component, representing 51% of the total area of the amide I′ band. The component located at 1651 cm^{-1} is usually assigned to α helix but, as in the case of the 1658 cm^{-1} component in the H_2O buffer, it may also correspond to large loops or turns with dihedral angles similar to those of α-helix [21, 31,51]. It is clear that the 1658 cm^{-1} component detected in the H_2O buffer (Table 4) did not include unordered structures since they would have shifted to a lower frequency of about 1643 cm^{-1} in D_2O buffer, but such a component was not detected [30]. The components located at 1662 (15%) and 1686 cm^{-1} (4%) arise from β-turns and the 1674 cm^{-1} band (9%) is usually assigned to antiparallel β-sheet structure [3, 32,33,52]. Quantitation of the secondary structure and assignments of the PKCε-C2 domain in D_2O are also summarized in Table 4 and will serve as a basis for the interpretation of temperature-dependent structural changes of the protein in D_2O buffer. Thus, there was very good agreement between the quantitation made in H_2O and in D_2O solutions, with 60% β-sheet being identified both in H_2O (adding the 1639 and 1689 cm^{-1} components) and D_2O (adding the 1636 and 1674 cm^{-1} components); 18% α-helix (or loops) in H_2O and 21% in D_2O and 22% β-turns (adding the 1686 and 1662 cm^{-1} components) in H_2O and 19% in D_2O.

A very good agreement was also reached between the secondary structure deduced from infrared spectroscopy and that concluded by means of X-ray diffraction from a crystal of this protein [55]. Table 2 shows that for β-pleated sheet the percentages found were 60% for infrared spectroscopy and 54% for X-ray diffraction (XRD), for α-helix 21% (IR) and 20% (XRD) and for β-turns 19% (IR) and 20% (XRD).

It is interesting that the 60% of β-sheet calculated for PKCε correlates also well with the percentages calculated by X-ray diffraction for C2 domains of the same topology, such as PLCδ (53%), cPLA2 (60%) and PKCδ-C2 (53%) domains [17,36,44]. Recent studies have shown the crystal structure of the PKCδ-C2 domain, which belongs to the group of novel PKCs. However, the low sequence homology between PKCε and PKCδ C2 domains suggests that further structural variations are expected to be found in this

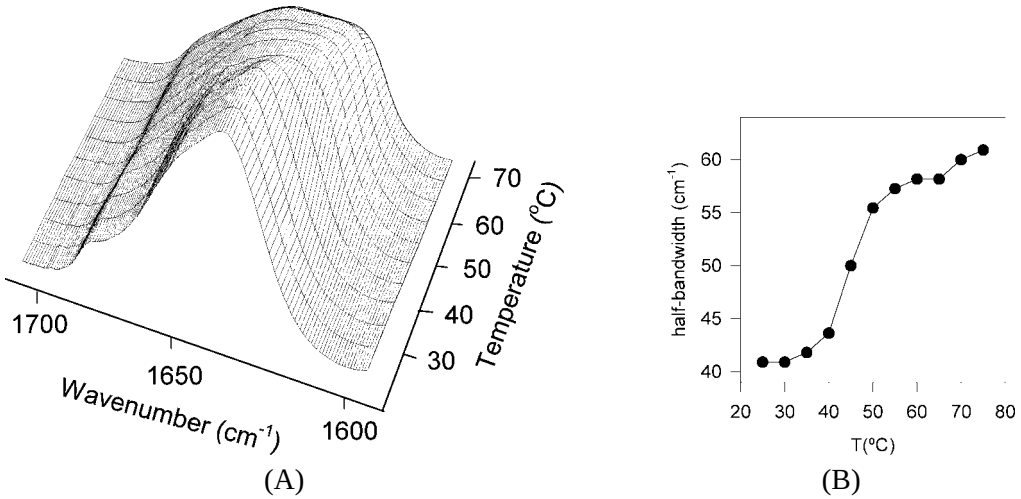

Fig. 6. (A) IR spectra of the PKCε-C2 domain in D_2O buffer containing 0.2 mM EGTA in the amide I′ region (1700–1600 cm^{-1}) as a function of temperature from 25 to 75°C. The increment of absorbance units (Δ) was 0.1. (B) Half-bandwidth of the amide I′ region of the IR spectra in cm^{-1} as a function of temperature, for the PKCε-C2 domain. Reproduced with permission from *Eur. J. Biochem.* **268** (2001), 1107–1117. Copyright 2001 Blackwell Sci.

group [17]. For example, there is an extended sequence in the CBR1-like loop of PKCε that could adopt a large loop conformation similar to that described in the CBR1 of PLCδ1, PTEN or PI3K [13,34,36]. Another possibility is that this part of the domain adopts a helical conformation similar to that of cPLA2-CBR1, which is involved in membrane interaction [44]. Thus, one of those structures may be the origin of the extra helical component found in the IR spectrum of PKCε-C2 domain at 1651 and 1658 cm^{-1}, in D_2O and H_2O, respectively, since both α-helix and large loops appear together at those frequencies [7, 28,53,54].

3.5. Study of the thermal stability of the PKCε-C2 domain by IR

Protein thermal denaturation can be followed using infrared spectroscopy by studying the temperature-induced changes produced in the amide I′ band. Protein thermal denaturation profiles are sensitive tools which reveal small conformational differences that are not always apparent from the individual infrared spectra.

The band decomposition procedure used in this work enabled us to analyse the thermally induced changes in protein structure in detail and the thermal behaviour of the individual structural elements. In general, large changes ($\geqslant$10 cm^{-1}) in band position seem to indicate variations in the secondary structure, whereas smaller shifts ($\leqslant$6 cm^{-1}) reflect local changes in a given conformation [31]. Figure 6A shows the pattern of PKCε-C2 domain upon heating, with the spectra basically revealing a typical broadening of the overall amide I′ contour [24,46,62]. Figure 6B depicts a plot of half-bandwidth versus temperature, which permitted the T_m transition temperature to be calculated (45°C approximately).

In order to study the thermal denaturation characteristics of this domain we have decomposed the different spectra into their constituents by curve-fitting. The number of components and positions were determined by previous deconvolution and derivation similarly to the spectra obtained at 25°C. The most significant changes compared with the spectrum recorded at 25°C (Fig. 5B) are the appearance of two new components at 1645 and 1622 cm^{-1} at 45°C, which gradually increased with increasing

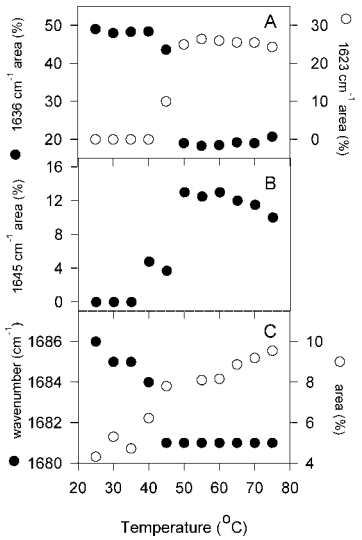

Fig. 7. Thermal profiles of the amide I′ components. (A) Percentage of band area detected at 1636 cm^{-1} (β-sheet) (●) and at 1623 cm^{-1} (aggregation) (○) versus temperature. (B) Percentage of band area detected at 1645 cm^{-1} (unordered) versus temperature. (C) Band position starting at 1680 cm^{-1} at 25°C (●) and percentage of band area of the same component (○) versus temperature. Reproduced with permission from *Eur. J. Biochem.* **268** (2001), 1107–1117. Copyright 2001 Blackwell Sci.

temperatures up to 60–80°C. The former can be attributed to an unordered structure [28] and the second to certain structures that arise upon thermal denaturation, such as extended chains not forming β-sheet (β-strands), irreversible aggregation or denaturated conformation [2,9,31,58].

An analysis of the peak positions, and the percentile areas of each component obtained by curve-fitting provided an idea of the secondary structural changes that occur during the thermal process. For example, the area of the component appearing at 1636 cm^{-1}, which has been attributed to β-sheet, abruptly decreased at 50°C from 49 to 19% (Fig. 7A). Furthermore, this decrease was correlated by an increasing in the percentage of the area of the 1622 cm^{-1} band from 0 to 25% at 50°C, suggesting that the emergence of the last component was a consequence of the process that induced the disappearance of the 1636 cm^{-1} component. Figure 7B shows the changes which occurred, with another new component appearing at 1644 cm^{-1} (assigned to unordered structure) and representing a maximum of 10–12% at the highest temperatures. This band seems to arise from the 1651 and 1636 cm^{-1} components that may be partially denaturated during the heating. A further significant change (Fig. 7C) concerned the component at 1686 cm^{-1}, which shifted to 1681 cm^{-1} at the same time that the percentage of its area increased from 4% at 25°C to 10% at 75°C [23]. These data suggest that there is only a small reorganization in the initial conformation of the β-turns, for example, the component at 1651 cm^{-1} slightly shifted to 1653 cm^{-1} at 40°C. Furthermore, the percentage of the area decreased from 21% at 25°C to 14% at 40°C and stayed constant during denaturation, indicating that this component, which is attributed to α-helix or large loops, is very stable during the heating process.

3.6. Effect of lipid binding on the structure of PKCε-C2 domain and its thermal denaturation pattern

IR was used to determine the effect of phosphatidic acid vesicles binding on the secondary structure of the PKCε-C2 domain. The spectrum was obtained and curve fitting was carried out for the PKCε-C2 domain bound to vesicles containing 100 mol% of phosphatidic acid in D_2O at 25°C in the 1780–

Table 5
Peak positions and assignment of the amide I and amide I′ bands of PKCε-C2 domain. Reproduced with permission from *Eur. J. Biochem.* **268** (2001), 1107–1117. Copyright 2001 Blackwell Sci.

H_2O				D_2O			
Position (cm^{-1})	Area (%)	Width (cm^{-1})	Assignment	Position (cm^{-1})	Area (%)	Width (cm^{-1})	Assignment
1689	9	19	Antiparallel β-sheet	1686	4	14	β-turns
1671	22	27	β-turns	1674	9	19	Antiparallel β-sheet
1658	18	23	α-helix, unordered structure or large loops	1662	15	20	β-turns
				1651	21	21	α-helix, large loops or turns with dihedral angles similar to α-helix
1639	51	31	β-sheet	1636	51	27	β-sheet

Table 6
Peak positions of the amide I′ band of PKCε-C2 domain bound to phosphatidic acid at 25 and 75°C. Reproduced with permission from *Eur. J. Biochem.* **268** (2001), 1107–1117. Copyright 2001 Blackwell Sci.

25°C			75°C		
Position (cm^{-1})	Area (%)	Width (cm^{-1})	Position (cm^{-1})	Area (%)	Width (cm^{-1})
1686	5	21	1686	8	30
1674	6	19	1673	10	21
1662	13	23	1662	15	21
1651	21	26	1650	19	24
1635	53	32	1635	48	36

1600 cm^{-1} region. The curve fitting data point to a secondary structure very similar to that obtained in the absence of lipids [23] which suggests that no differences or changes in the secondary structure occur when lipid binding takes place. It is interesting to note that these results are different from those observed for the PKCα-C2 domain, which showed an increase in the component representing unordered and open loop structures upon lipid binding [24].

The effect of heating on the secondary structure of PKCε-C2 in the presence of phosphatidic acid was also followed by IR. The heating profile showed few changes in the temperature range that was studied. To better characterize these changes, the spectrum obtained at 75°C was analyzed by curve fitting (Table 6), which revealed that the component at 1635 cm^{-1} decreased to 48% of the total area (from 53% at 25°C). Nevertheless, if we consider the contribution of the 1674 cm^{-1} band, the total percentage of the β-sheet components was 58%, which implies that no significant changes took place with this heating process, since it amounted to 60% at 25°C. The other components were very similar to those obtained at 25°C (Table 5), suggesting that in the presence of phosphatidic acid, the heating process carried out here produced only slight modifications in the secondary structure under our experimental conditions.

3.7. Comparison of C2 from PKCα and C2 from PKCε

Some significant differences were observed between both C2 domains, knowing that whereas the C2 domain from PKCα has a type I topology, the C2 from PKCε has a type II topology. It is interesting to note that in spite of sharing a core β-sheet with many other C2 domains, including the PKCα-C2 domain, IR detected significant differences between this last domain and the PKCε-C2 [23,24]. For example, the component at 1644 cm^{-1} assigned to open loops and unordered structure in the PKCα-C2 cannot be found in the PKCε-C2 domain. Moreover, the band at 1651 cm^{-1} which is attributed to α-helix or large loops, is significantly greater in the PKCε-C2 in D_2O solution (21%) than in PKCα-C2 (12%).

The effect of lipid binding was also different, so that it induced a well detectable change in C2 from PKCα but very little change was appreciated for the C2 of PKCε.

With respect to thermal stability, it has been shown that in PKCα-C2 domain, the unordered structures and those components characteristic of thermal denaturation (1646, 1625 and 1680 cm^{-1}) increase substantially at 75°C, a finding which correlates well with the decrease observed in the percentage of the α-helical and β-sheet components [24]. On the other hand, the PKCε-C2 domain retains the 1651 cm^{-1} component and part of the β-sheet structure after heating. These results demonstrate that the PKCε-C2 domain is more stable than the PKCα-C2 domain in the absence of Ca^{2+}. These results support the idea that one of Ca^{2+} functions is to stabilize the domain before lipid binding and thus, in the cases where the function of the C2 domain is independent of calcium this role is played by the protein itself. Furthermore, many studies of the C2 domains of topology II, such as cPLA2, have demonstrated that CBR1 and CBR3 contain hydrophobic residues that are very important for membrane binding [35,43]. The homologous residues of PKCε-C2 domain, which contribute to CBR1 and CBR3, could be potential candidates for the absorbance seen at this particular wavelength (1651 cm^{-1}). These results suggest that the PKCε-C2 domain possesses a more ordered secondary structure than other C2 domains, which may be due to the connecting loops since the core β-sheet is similar in all C2 domains.

The C2 domains of novel PKCs constitute a special case since they have been classified as topology II although their membrane binding capacity depends on acidic phospholipids in a Ca^{2+}-independent way [15]. It has been demonstrated recently that PKCε, due to the lack of Ca^{2+} binding, interacts with low specificity with PS and DAG, which implies the presence of other physiological activators for this form [39]. For example, it is well established that PLD activation induces an increase of phosphatidic acid in biological membranes [27] and this could be a way of activating PKCε. As it was demonstrated previously [23] the PKCε-C2 domain has an important affinity for phosphatidic acid vesicles although the secondary structure of the domain did not change upon lipid binding, in contrast with PKCα-C2 domain that underwent significant changes ([23] and this work). These results correlate well with the need for the PKCα to penetrate the membrane to be fully activated, the result of which could be the structural reorganization seen by IR. Experiments on phospholipid monolayer penetration, on the other hand, have revealed that PKCε penetrates the membrane to a lesser extent than PKCα. This might result in no secondary structural reorganization upon lipid binding, although some reorganization at the tertiary level cannot be discarded [39].

Acknowledgements

We are very grateful to Dr. Ono and Dr. Nishizuka (Kobe University, Japan) for the kind gift of the cDNA codifying PKCε. This work was supported by Grant PB98-0389 from Dirección General de Enseñanza Superior e Investigación Científica (Spain) and by Grant PI-35/00789/FS/01 from Fundación Séneca (Murcia).

References

[1] A. Dessen, J. Tang, H. Schmidt, M. Stahl, J.D. Clark, J. Seehra and W.S. Somers, Crystal structure of human cytosolic phospholipase A2 reveals a novel topology and catalytic mechanism, *Cell* **97** (1999), 349–360.

[2] A. Martinez, J. Haavik, T. Flatmark, J.L.R. Arrondo and A. Muga, Conformational properties and stability of tyrosine hydroxylase studied by infrared spectroscopy. Effect of iron/catecholamine binding and phosphorylation, *J. Biol. Chem.* **271** (1996), 19 737–19 742.

[3] A. Muga, J.L.R. Arrondo, T. Bellon, J. Sancho and C. Bernabeu, Structural and functional studies on the interaction of sodium dodecyl sulfate with beta-galactosidase, *Arch. Biochem. Biophys.* **300** (1993), 451–455.

[4] A. Newton and J.E. Johnson, Protein kinase C: a paradigm for regulation of protein function by two membrane-targeting modules, *Biochim. Biophys. Acta* **1376** (1998), 155–172.

[5] A.S. Edwards and A.C. Newton, Regulation of protein kinase C βII by its C2 domain, *Biochemistry* **36** (1997), 15 615–15 623.

[6] B.A. Davletov and T.C. Südhof, A single C2 domain from synaptotagmin I is sufficient for high affinity Ca^{2+}/phospholipid binding, *J. Biol. Chem.* **268** (1993), 26 386–26 390.

[7] C.L. Wilder, A.D. Friedrich, R.O. Potts, G.O. Daumy and M.L. Francoeur, Secondary structural analysis of two recombinant murine proteins, interleukins 1 alpha and 1 beta: is infrared spectroscopy sufficient to assign structure?, *Biochemistry* **31** (1992), 27–31.

[8] D. Chapman, M. Jackson and P.I. Haris, Investigation of membrane protein structure using Fourier transform infrared spectroscopy, *Biochem. Soc. Trans.* **17** (1989), 617–619.

[9] D. Naumann, C. Schultz, U. Görne-Tschelnokow and F. Hucho, Secondary structure and temperature behavior of the acetylcholine receptor by Fourier transform infrared spectroscopy, *Biochemistry* **32** (1993), 3162–3169.

[10] D.M. Byler and H. Susi, Examination of the secondary structure of proteins by deconvolved FTIR spectra, *Biopolymers* **25** (1986), 469–487.

[11] E.A. Nalefski and J.J. Falke, The C2 domain calcium-binding motif: structural and functional diversity, *Protein Science* **5** (1996), 2375–2390.

[12] E.A. Nalefski, M.M. Slazas and J.J. Falke, Calcium signaling cycle of a membrane-docking C2 domain, *Biochemistry* **36** (1997), 12 011–12 018.

[13] E.H. Walker, O. Perisic, C. Rled, L. Stephens and R.L. Williams, Structural insights into phosphoinositide 3-kinase catalysis and signalling, *Nature* **402** (1999), 313–320.

[14] H. Fabian, D. Naumann, R. Misselwitz, O. Ristau, D. Gerlach and H. Welfle, Secondary structure of streptokinase in aqueous solution: a Fourier transform infrared spectroscopic study, *Biochemistry* **31** (1992), 6532–6538.

[15] H. Koide, K. Ogita, U. Kikkawa and Y. Nishizuka, Isolation and characterization of the epsilon subspecies of protein kinase C from rat brain, *Proc. Natl. Acad. Sci. USA* **89** (1992), 1149–1153.

[16] H. Mellor and P.J. Parker, The extended protein kinase C superfamily, *Biochem. J.* **332** (1998), 281–292.

[17] H. Pappa, J. Murray-Rust, L.V. Dekker, P.J. Parker and N.Q. McDonald, Crystal structure of the C2 domain from protein kinase Cδ, *Structure* **6** (1998), 885–894.

[18] H. Susi, Infrared spectroscopy-conformation, *Methods Enzymol.* **26** (1972), 455–472.

[19] H. Zhang, Y. Ishikawa, Y. Yamamoto and R. Carpentier, Secondary structure of streptokinase in aqueous solution: a Fourier transform infrared spectroscopic study, *FEBS Letters* **426** (1998), 347–351.

[20] J. Bandekar and S. Krimm, Vibrational analysis of peptides, polypeptides, and proteins. VI. Assignment of beta-turn modes in insulin and other proteins, *Biopolymers* **19** (1980), 31–36.

[21] J. Bandekar, Amide modes and protein conformation, *Biochim. Biophys. Acta* **1120** (1992), 123–143.

[22] J. Cladera, H.L. Galisteo, M. Sabes, P.L. Mateo and E. Padros, The role of retinal in the thermal stability of the purple membrane, *Eur. J. Biochem.* **207** (1992), 581–585.

[23] J. García-García, J.C. Gómez-Fernández and S. Corbalán-García, Structural characterization of the C2 domain of novel protein kinase Cε, *Eur. J. Biochem.* **268** (2001), 1107–1117.

[24] J. García-García, S. Corbalán-García and J.C. Gómez-Fernández, Effect of calcium and phosphatidic acid binding on the C2 domain of PKCα as studied by Fourier transform infrared spectroscopy, *Biochemistry* **38** (1999), 9667–9675.

[25] J. Hofmann, The potential for isoenzyme-selective modulation of protein kinase C, *FASEB J.* **11** (1997), 649–669.

[26] J. Rizo and T.C. Südhof, C2-domains, structure and function of a universal Ca^{2+}-binding domain, *J. Biol. Chem.* **273** (1998), 15 879–15 882.

[27] J.H. Exton, New developments in phospholipase D, *J. Biol. Chem.* **272** (1997), 15 579–15 582.

[28] J.L.R. Arrondo and F.M. Goñi, Structure and dynamics of membrane proteins as studied by infrared spectroscopy, *Prog. Biophys. Mol. Biol.* **72** (1999), 367–405.

[29] J.L.R. Arrondo, A. Muga, J. Castresana, C. Bernabeu and F.M. Goñi, An infrared spectroscopic study of β-galactosidase structure in aqueous solutions, *FEBS Letters* **252** (1989), 118–120.

[30] J.L.R. Arrondo, I. Etxabe, U. Dornberger and F.M. Goñi, Probing protein conformation by infrared spectroscopy, *Biochem. Soc. Trans.* **22** (1994), 380S.
[31] J.L.R. Arrondo, J. Castresana, J.M. Valpuesta and F.M. Goñi, Structure and thermal denaturation of crystalline and non-crystalline cytochrome oxidase as studied by infrared spectroscopy, *Biochemistry* **33** (1994), 11 650–11 655.
[32] J.L.R. Arrondo, A. Muga, J. Castresana and F.M. Goñi, Quantitative studies of the structure of proteins in solution by Fourier-transform infrared spectroscopy, *Prog. Biophys. Mol. Biol.* **59** (1993), 23–56.
[33] J.M. Olinger, D.M. Hill, R.J. Jakobsen and R.S. Brody, Fourier transform infrared studies of ribonuclease in H_2O and ^2H_2O solutions, *Biochim. Biophys. Acta* **869** (1986), 89–98.
[34] J.O. Lee, H. Yang, M.-M. Georgescu, A.D. Cristofano, T. Maehama, Y. Shi, J.E. Dixon, P. Pandolfi and N.P. Pavletich, Crystal structure of the PTEN tumor suppressor: implications for its phosphoinositide phosphatase activity and membrane association, *Cell* **99** (1999), 323–334.
[35] L. Bittova, M. Sumandea and W. Cho, A structure-function study of the C2 domain of cytosolic phospholipase A2, *J. Biol. Chem.* **274** (1999), 9665–9672.
[36] L.O. Essen, O. Perisic, R. Cheung, M. Katan and R.L. Williams, Crystal structure of a mammalian phosphoinositide-specific phospholipase Cδ, *Nature* **380** (1996), 595–602.
[37] M. Gonzalez, L.A. Bagatolli, I. Echabe, J.L.R. Arrondo, C.E. Argaraña, C.R. Cantor and G.D. Fidelio, *J. Biol. Chem.* **272** (1997), 11 288–11 294.
[38] M. Jackson, P.I. Haris and D. Chapman, Fourier transform infrared spectroscopic studies of Ca^{2+}-binding proteins, *Biochemistry* **30** (1991), 9681–9686.
[39] M. Medkova and W. Cho, Differential membrane-binding and activation mechanisms of protein kinase Cα and ε, *Biochemistry* **37** (1998), 4892–4900.
[40] M. Medkova and W. Cho, Interplay of C1 and C2 domains of protein kinase C-alpha in its membrane binding and activation, *J. Biol. Chem.* **274** (1999), 19 852–19 861.
[41] M. Medkova and W. Cho, Mutagenesis of the C2 domain of protein kinase Cα, *J. Biol. Chem.* **273** (1998), 17 544–17 552.
[42] N. Verdaguer, S. Corbalán-García, W.F. Ochoa, I. Fita and J.C. Gómez-Fernández, Ca^{2+} bridges the C2 membrane-binding domain of protein kinase Cα directly to phosphatidylserine, *EMBO J.* **18** (1999), 6329–6338.
[43] O. Perisic, H.F. Paterson, G. Mosedale, S. Lara-Gonzalez and R.L. Williams, Mapping the phospholipid-binding surface and translocation determinants of the C2 domain from cytosolic phospholipase A2, *J. Biol. Chem.* **274** (1999), 14 979–14 987.
[44] O. Perisic, S. Fong, D.E. Lynch, M. Bycroft and R.L. Williams, Crystal structure of a calcium–phospholipid binding domain from cytosolic phospholipase A2, *J. Biol. Chem.* **273** (1998), 1596–1604.
[45] P.J. Plant, H. Yeger, O. Staub, P. Howard and D. Rotin, The C2 domain of the ubiquitin protein ligase Nedd4 mediates Ca^{2+}-dependent plasma membrane localization, *J. Biol. Chem.* **272** (1997), 32 329–32 336.
[46] R. Chehin, Y. Iloro, M.J. Marcos, E. Villar, V.L. Shnyrov and J.L.R. Arrondo, Thermal and pH-induced conformational changes of a beta-sheet protein monitored by infrared spectroscopy, *Biochemistry* **38** (1999), 1525–1530.
[47] R.B. Sutton and S.R. Sprang, Structure of the protein kinase Cβ phospholipid-binding C2 domain complexed with Ca^{2+}, *Structure* **6** (1998), 1395–1405.
[48] R.B. Sutton, B.A. Davletov, A.M. Berghuis, T.C. Südhof and S.R. Sprang, Structure of the first C2 domain of synaptotagmin I: a novel Ca^{2+}/phospholipid-binding fold, *Cell* **80** (1995), 929–938.
[49] S. Corbalán-García, J.A. Rodríguez-Alfaro and J.C. Gómez-Fernández, Determination of the calcium-binding sites of the C2 domain of protein kinase Cα that are critical for its translocation to the plasma membrane, *Biochem. J.* **337** (1999), 513–521.
[50] S. Corbalán-García, J.A. Teruel, J. Villalaín and J.C. Gómez-Fernández, Extensive proteolytic digestion of the (Ca^{2+}-Mg^{2+})-ATPase from sarcoplasmic reticulum leads to a highly hydrophobic proteinaceous residue with a mainly alpha-helical structure, *Biochemistry* **33** (1994), 8247–8254.
[51] S. Krim and J. Bandekar, Vibrational spectroscopy and conformation of peptides, polypeptides, and proteins, *Adv. Protein Chem.* **38** (1986), 181–364.
[52] S.A. Tatuliam, D.M. Cortes and E. Perozo, Structural dynamics of the Streptomyces lividans K^+ channel (SKC1): secondary structure characterization from FTIR spectroscopy, *FEBS Lett.* **423** (1998), 205–212.
[53] S.J. Prestelski, D.M. Byler and M.N. Liebman, Comparison of various molecular forms of bovine trypsin: correlation of infrared spectra with X-ray crystal structures, *Biochemistry* **30** (1991), 133–143.
[54] S.L. Prestrelski, T. Arakawa, W.C. Kenney and D.M. Byler, The secondary structure of two recombinant human growth factors, platelet-derived growth factor and basic fibroblast growth factor, as determined by Fourier-transform infrared spectroscopy, *Archiv. Biochem. Biophys.* **285** (1991), 111–115.
[55] W.F. Ochoa, J. García-García, I. Fita, S. Corbalán-García, N. Verdaguer and J.C. Gómez-Fernández, Structure of the C2 domain from novel protein kinase Cε. A membrane binding model for Ca^{2+}-independent C2 domains, *J. Mol. Biol.* **311** (2001), 837–849.
[56] W.F. Ochoa, S. Corbalán-García, R. Eritja, J.A. Rodríguez-Alfaro, J.C. Gómez-Fernández, I. Fita and N. Verdaguer, Ad-

ditional binding sites for anionic phospholipids and calcium ions in the crystal structures of complexes of the C2 domain of protein kinase Cα, *J. Mol. Biol.* (2002), in press.
[57] W.K. Surewicz, H.H. Mantsch and D. Chapman, Determination of protein secondary structure by Fourier transform infrared spectroscopy: a critical assessment, *Biochemistry* **32** (1993), 389–394.
[58] W.K. Surewicz, J.J. Leddy and H.H. Mantsch, Structure, stability, and receptor interaction of cholera toxin as studied by Fourier-transform infrared spectroscopy, *Biochemistry* **29** (1990), 8106–8111.
[59] W.K. Surewicz, T.M. Stepanik, A.G. Szabo and H.H. Mantsch, Lipid-induced changes in the secondary structure of snake venom cardiotoxins, *J. Biol. Chem.* **263** (1988), 786–790.
[60] W. Orr, L.M. Keranen and A.C. Newton, Reversible exposure of the pseudosubstrate domain of protein kinase C by phosphatidylserine and diacylglycerol, *J. Biol. Chem.* **267** (1992), 15 263–15 266.
[61] J.W. Orr and A.C. Newton, Interaction of protein kinase C with phosphatidylserine: 2. Specificity and regulation, *Biochemistry* **31** (1992), 4667–4673.
[62] X. Hang, G. Li, G. Li and K. Lin, FTIR study of the thermal denaturation of alpha-actinin in its lipid-free and dioleoylphosphatidylglycerol-bound states and the central and N-terminal domains of alpha-actinin in D_2O, *Biochemistry* **37** (1998), 10 730–10 737.
[63] X. Shao, B.A. Davletov, R.B. Sutton, T.C. Südhof and J. Rizo, Bipartite Ca^{2+} binding motif in C2 domains of synaptotagmin and PKC, *Science* **273** (1996), 248–251.
[64] X. Shao, Y. Fernandez, T.C. Südhof and J. Rizo, Solution structures of the Ca^{2+}-free and Ca^{2+}-bound C2A domain of synaptotagmin I: does Ca^{2+} induce a conformational change?, *Biochemistry* **37** (1998), 16 106–16 115.
[65] Y. Echabe, U. Dornberger, A. Prado, F.M. Goñi and J.L.R. Arrondo, Topology of sarcoplasmic reticulum Ca^{2+}-ATPase: an infrared study of thermal denaturation and limited proteolysis, *Protein Sci.* **7** (1998), 1172–1179.
[66] Y. Nishizuka, Protein kinase C and lipid signaling for sustained cellular responses, *FASEB J.* **9** (1995), 484–496.